Supplementary Material

A bottom-up design strategy for controllable self-assembly based on the isotropic double-well potential

Youyuan Zhu[a,b], Yijun Bai[a], Hao Dong[a,c,d],*, Wei Wang[b,c],*

[a] Kuang Yaming Honors School, Nanjing University, Nanjing 210023, China;
[b] Collaborative Innovation Center of Advanced Microstructures, National Laboratory of Solid State Microstructure, & Department of Physics, Nanjing University, Nanjing 210093, China;
[c] Institute for Brain Sciences, Nanjing University, Nanjing 210023, China.
[d] State Key Laboratory of Analytical Chemistry for Life Science, Nanjing University, Nanjing 210023, China.

Correspondence: donghao@nju.edu.cn, wangwei@nju.edu.cn

Aggregation dynamics of **pattern II** have been described in the manuscript (**Figure 2**). Now, we discuss the other four patterns of aggregation.

We take T=0.6 as an example for **pattern I**. The aggregation of particles is roughly divided into three states: particles gather, clusters merge and fine-tuning of the cluster structure (**Figure S1**). First, cluster-2.0 gradually forms by the interaction of W_O (**Figure S1a**). The rapid decrease in the number of clusters-2.0 and the increase in particles in W_O indicate that clusters absorbed free particles by the interaction of W_O. After that, clusters merge so that the maximum size of cluster-2.0 increases discretely (**Figure S1a**). A high slope of the curve corresponds to cluster merging (**Figure S1b**). Finally, the structure of the aggregates does not undergo significant changes for a long time. There are almost no particles in W_I during aggregation. Particles cannot crossover the barrier because of the low temperature. The ratio of the maximum size of clusters-2.0 and 1.2 and the number of particles in W_O and W_I (**Figure S1c**) are over 100 most of the time. This means that the system is loosely packed by the interaction of W_O.

We take T=4 as an example for **pattern III**. Similar three states can be observed. First, the maximum size and number of clusters-2.0 and 1.2 almost change identically, while particles in the W_I increase gradually to saturation (**Figure S2a**). This indicates that clusters absorbed free particles by the interaction of W_I directly. Then, clusters merge. Particles can crossover the barrier and form clusters by the interaction of W_I directly because of the increase in temperature. The discrete increase in the maximum size of clusters and the high slope of the cluster number in **Figure S2b** correspond to cluster merging. The system becomes close-packed as the ratio of the maximum size of clusters converges to 1 (**Figure S2c**). The ratio of the number of particles initially decreases, then increases and finally converges to a constant. This means that particles initially form small close-packed clusters and then clusters merge.

We take T=8 as an example of **pattern IV**. The three states of aggregation are similar to those of **pattern III** (**Figure S3a**). However, clusters absorbed free particles by the interaction of W_I much more slowly because small clusters are unstable. The cluster merges first and then tunes the local structure (**Figure S3b**). A longer duration of convergence corresponds to longer absorption (**Figure S3c**). A decrease in the number of free particles leads to a decrease in the ratio of the number of particles (**Figure S3c**).

When the temperature is very high, all particles are in a mess (**pattern V**). All values fluctuate with time (**Figure S4**, T=9).

A single-well LJ potential forms fcc structure (**Figure S5**).

The cell parameters and radial distribution function of identified structures by LJG potentials are shown in **Table S1** and **Figure S6**.
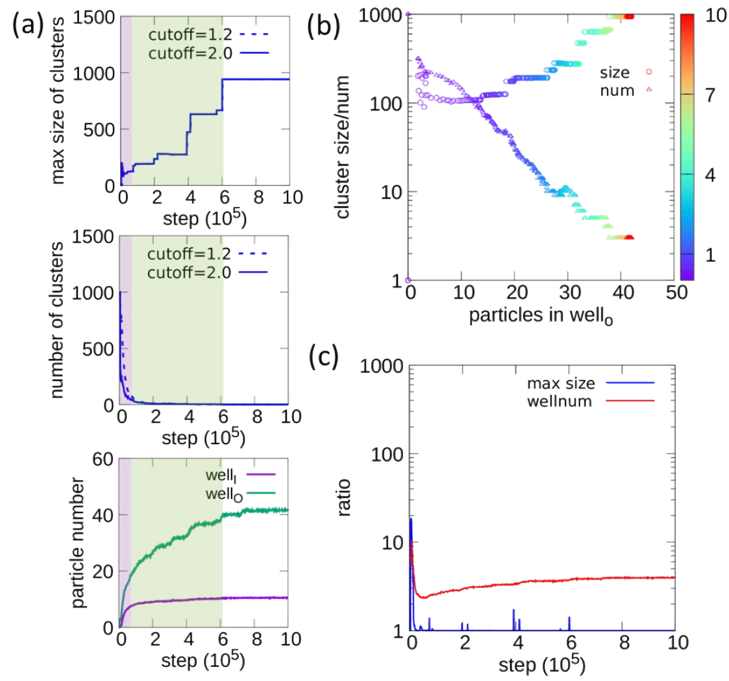
Table S1. Information of identified structures by LJG potentials

Type	Pearson symbol	Cell parameters	Primitive translation vectors	Particle coordinates in primitive cell
T1	cI2	$\alpha=\beta=\gamma=90°$ $a=b=c=0.90*$	$(\sqrt{2}x,x,0)$ $(0,2x,0)$ $(0,x,\sqrt{2}x)$ $x=0.64$	$(0,0,0)$
T3	tI4	$\alpha=\beta=\gamma=90°$ $a=b=1.51,$ $c=0.88$	$(x,0,0)$ $(0,\sqrt{3}x,0)$ $(\frac{x}{2},\frac{\sqrt{3}}{2}x,\frac{\sqrt{3}}{2}x)$ $x=0.88$	$(0,0,0)$ $(\frac{x}{4},\frac{\sqrt{3}}{2}x,0)$
T4	cI12	$\alpha=\beta=\gamma=90°,$ $a=b=c=1.64$	$(x,\sqrt{2}x,0)$ $(-x,\sqrt{2}x,0)$ $(x,0,\sqrt{2}x)$ $x=0.82$	$(0,0,0)$ $\left(-\frac{x}{2}+\frac{\sqrt{6}}{8}x,\frac{5\sqrt{2}}{8}x,\frac{\sqrt{2}}{8}x\right)$ $\left(0,\frac{5\sqrt{2}}{4}x,\frac{\sqrt{2}}{4}x\right)$ $\left(\frac{x}{2},\frac{3\sqrt{2}}{4}x,\frac{\sqrt{2}}{2}x\right)$ $\left(\frac{x}{2},\frac{3\sqrt{2}}{2}x,\frac{3\sqrt{2}}{4}x\right)$ $(x+\frac{\sqrt{6}}{8}x,\frac{9\sqrt{2}}{8}x,\frac{5\sqrt{2}}{8}x)$
T5	oF8	$\alpha=\beta=\gamma=90°,$ $a=0.90,\ \ b=1.22,$ $c=2.76$	$(-x,y,0)$ $(-x,-y,0)$ $(-x,0,z)$ $x=0.46,y=0.62,z=1.39$	$(0,0,0)$ $(-\frac{3}{2}x,\frac{y}{2},\frac{z}{2})$
T6	hP2	$\alpha=\beta=90°,$ $\gamma=120°$ $a=b=0.79,$ $c=1.17$	$(-\frac{x}{2},\frac{\sqrt{3}}{2}x,0)$ $(-\frac{x}{2},-\frac{\sqrt{3}}{2}x,0)$ $(0,0,y)$ $x=0.79,y=1.17$	$(0,0,0)$ $\left(-\frac{x}{2},\frac{\sqrt{3}}{6}x,\frac{y}{2}\right)$
T7	cF4	$\alpha=\beta=\gamma=90°,$ $a=b=c=1.16$	$(\frac{x}{2},\frac{\sqrt{3}}{2}x,0)$ $(0,\sqrt{3}x,0)$ $\left(0,\frac{\sqrt{3}}{3}x,\frac{\sqrt{6}}{3}x\right)$	$(0,0,0)$

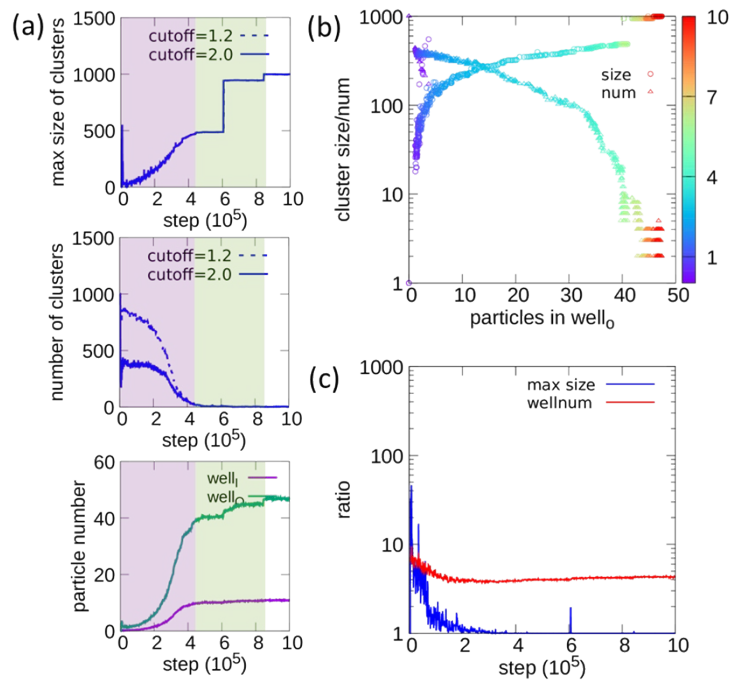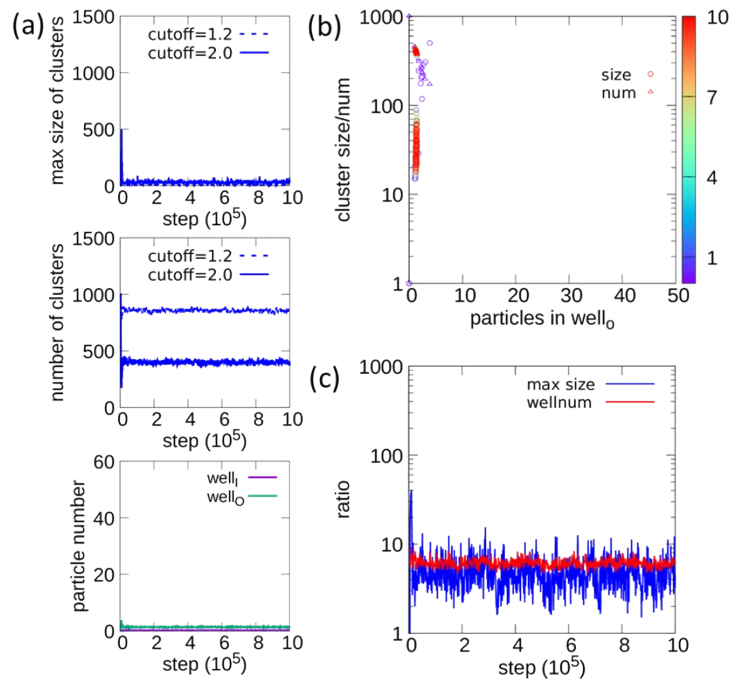|				
			x=0.82	
T8	tI2	$\alpha=\beta=\gamma=90°$ a=b=0.99, c=0.76	$(x,y,0)$ $(-x,y,0)$ $(0,y,x)$ x=0.71,y=0.38	$(0,0,0)$
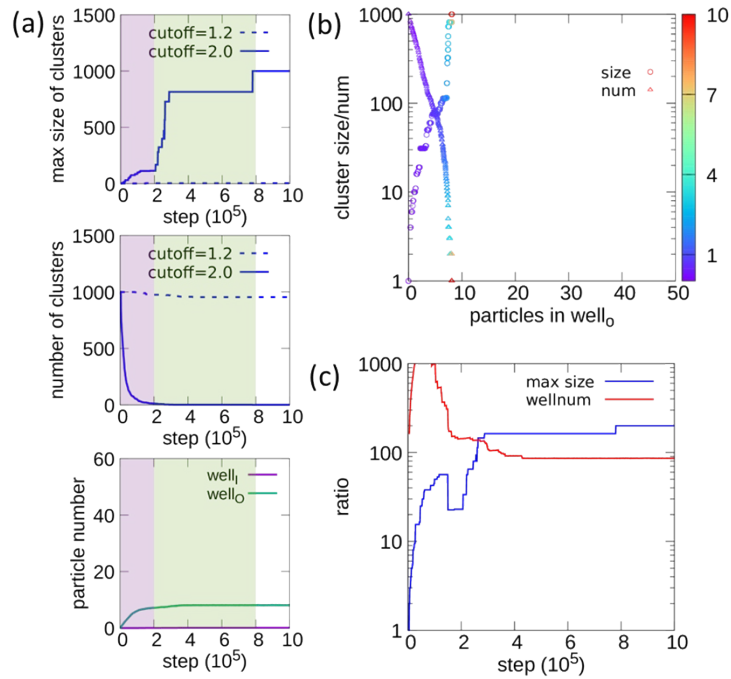
Figure S1. Aggregation dynamic processes of pattern I guided by OP (I = 10, J = 10, K = 0) at T=0.1. (a) The max size of a cluster in the system (top), the number of clusters (middle), and the number of particles characterized by the position of two wells on the potential (bottom). In each panel, three aggregation states are colored in sequence, namely particle aggregation (purple), cluster merging (light green) and fine-tuning of the cluster structure (white). The tightly packed cluster-1.2 and the loosely packed cluster-2.0 are shown using dashed and solid lines. (b) The correlation between the max size and number of clusters and the number of particles in the well. Color represents time steps whose unit is 100 thousand steps. The y-axes are in log scale. (c) The ratio of the max size of cluster-2.0 and cluster-1.2 and the number of particles in W_O and W_I. The y-axes are in log scale.

Figure S2. Aggregation dynamic processes of pattern III guided by OP (I = 10, J = 10, K = 0) at T=4. (a) The max size of a cluster in the system (top), the number of clusters (middle), and the number of particles characterized by the position of two wells on the potential (bottom). In each panel, three aggregation states are colored in sequence, namely particle aggregation (purple), cluster merging (light green) and fine-tuning of the cluster structure (white). The tightly packed cluster-1.2 and the loosely packed cluster-2.0 are shown using dashed and solid lines. (b) The correlation between the max size and number of clusters and the number of particles in the well. Color represents time steps whose unit is 100 thousand steps. The y-axes are in log scale. (c) The ratio of the max size of cluster-2.0 and cluster-1.2 and the number of particles in W_O and W_I. The y-axes are in log scale.

Figure S3. Aggregation dynamic processes of pattern IV guided by OP (I = 10, J = 10, K = 0) at T=8. (a) The max size of a cluster in the system (top), the number of clusters (middle), and the number of particles characterized by the position of two wells on the potential (bottom). In each panel, three aggregation states are colored in sequence, namely particle aggregation (purple), cluster merging (light green) and fine-tuning of the cluster structure (white). The tightly packed cluster-1.2 and the loosely packed cluster-2.0 are shown using dashed and solid lines. (b) The correlation between the max size and number of clusters and the number of particles in the well. Color represents time steps whose unit is 100 thousand steps. The y-axes are in log scale. (c) The ratio of the max size of cluster-2.0 and cluster-1.2 and the number of particles in W_O and W_I. The y-axes are in log scale.

Figure S4. Aggregation dynamic processes of pattern V guided by OP (I = 10, J = 10, K = 0) at T=9. (a) The max size of a cluster in the system (top), the number of clusters (middle), and the number of particles characterized by the position of two wells on the potential (bottom). The tightly packed cluster-1.2 and loosely packed cluster-2.0 are shown using dashed and solid lines. (b) The correlation between the max size and number of clusters and the number of particles in the well. Color represents time steps whose unit is 100 thousand steps. The y-axes are in log scale. (c) The ratio of the max size of cluster-2.0 and cluster-1.2 and the number of particles in W_O and W_I. The y-axes are in log scale.
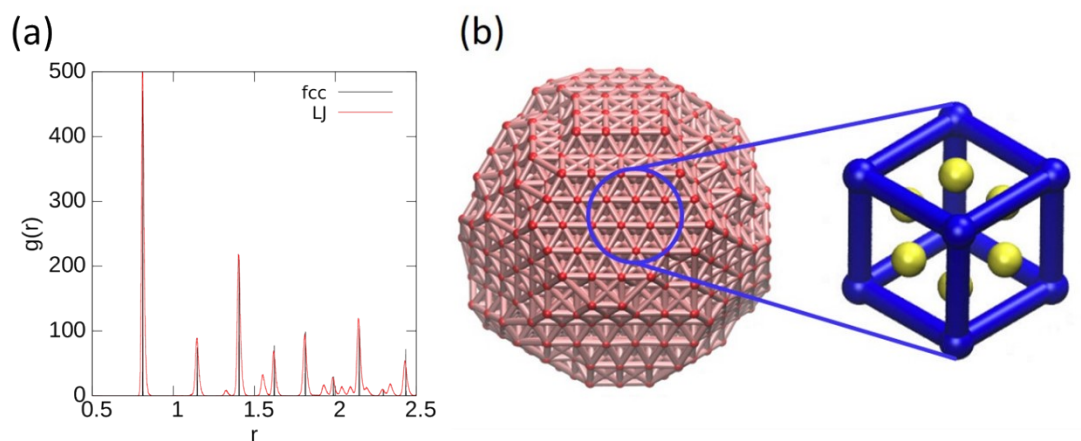
Figure S5. The formation of the fcc configuration of 1000 particles guided by a single-well Leonard-Jones potential. (a) The radial distribution function of the system (red line) and a standard fcc crystal with the lattice parameters α=β=γ=90°, a=b=c=1.16 (blue). (b) The self-assembled structure with the unit cell highlighted.
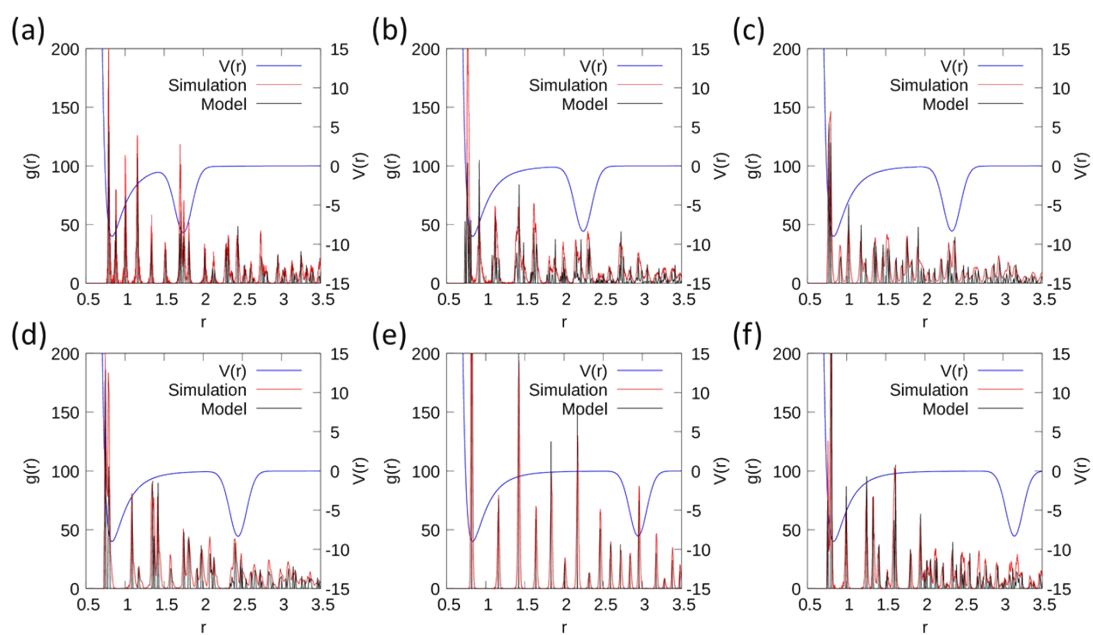
Figure S6. The distribution function of 6 identified structures by LJG potentials. (a)-(f) correspond to the configurations of **T3** to **T8**. The potential function profiles are plotted in blue, and the distribution function of simulated structures and model by identification are plotted in red and black, respectively.